American Mineralogist, Volume 87, pages 1528–1535, 2002

Interpretation of K-Ar dates of illitic clays from sedimentary rocks aided by modeling

JAN ŚRODOŃ,[1,*] NORBERT CLAUER,[2] AND DENNIS D.D. EBERL[3]

[1]Institute of Geological Sciences PAN, Senacka 1, 31-002 Kraków, Poland
[2]Centre de Geochimie de la Surface CNRS-ULP, 1, rue Blessig, 67084 Strasbourg, France
[3]U.S. Geological Survey, 3215 Marine St., Suite E-127, Boulder, Colorado 80303-1066, U.S.A.

ABSTRACT

K-Ar dates of illitic clays from sedimentary rocks may contain "mixed ages," i.e., may have ages that are intermediate between the ages of end-member events. Two phenomena that may cause mixed ages are: (1) long-lasting reaction during the burial illitization of smectite; and (2) physical mixing of detrital and diagenetic components. The first phenomenon was investigated by simulation of illitization reactions using a nucleation and growth mechanism. These calculations indicate that values for mixed ages are related to burial history: for an equivalent length of reaction time, fast burial followed by slow burial produces much older mixed ages than slow burial followed by fast. The type of reaction that occurred in a rock can be determined from the distribution of ages with respect to the thickness of illite crystals. Dating of artificial mixtures confirms a non-linear relation between mixed ages and the proportions of the components. Vertical variation of K-Ar age dates from Gulf Coast shales can be modeled by assuming diagenetic illitization that overprints a subtle vertical trend (presumably of sedimentary origin) in detrital mineral content.

INTRODUCTION

The crystallization of illite has been recognized as a major and widespread post-sedimentary reaction in detrital sediments (see Środoń 1999a for a recent review). Consequently, K-Ar dating of illite is an important tool for finding the ages of diagenetic and low-temperature metamorphic events (reviewed by Clauer and Chaudhuri 1995).

K-Ar dating of illitic clays is not much different from dating other K-bearing minerals. Previous concerns about Ar diffusion from small illite particles have been addressed by many authors (e.g., Aronson and Lee 1986; Hunzicker et al. 1986; Clauer et al. 1997 and literature cited therein) and were found to be unimportant in the temperature range of diagenesis and anchimetamorphism. Only the low K content of some clays (randomly interstratified illite-smectite) and the presence of organic material in the clay fraction pose specific analytical difficulties.

The real challenge in dating illite and illite-smectite is in matching the measured dates to the geological events during which the illitization occurred. Two phenomena make such interpretations difficult: (1) The specific nature of the smectite illitization reaction, which, in sediments, usually is not a single event, but is a reaction that continues over a broad temperature range, through burial diagenesis and anchimetamorphism (ca., 70 to 300 °C; reviewed recently by Środoń 1999a); and (2) The detrital contamination of even the finest clay fractions of common sedimentary rocks (Clauer et al. 1997).

Because the burial of sedimentary rocks often is a long-lasting process, extending over millions or tens of millions of years, the ages of most sedimentary illites, even those free of detrital contamination (e.g., from bentonites), have to be treated as "mixed ages," i.e., as values intermediate between the ages of end-member events.

Several authors have attempted to extract pure end-member ages from mixed ages (e.g., Aronson and Hower 1976; Mossman 1991; Pevear 1992). This specific aspect of illite dating also has been considered by the present authors (Clauer et al. 1997; Chaudhuri et al.1999; Środoń 1999b, 2000). The present contribution offers a more comprehensive treatment of these problems. It is based on an approach to dating mixtures developed by Środoń (1999b, 2000) and discussed by Ylagan et al. (2000), which recognizes that, for purely mathematical reasons (a ratio and a logarithm in the age equation), a mixed age is not the mean of the end-member ages. Thus the linear technique of extrapolating end-member ages from a series of mixed ages (which is equivalent to considering the mixed age as a mean age) should not be used. Instead, mixed ages can be calculated by putting mean K and mean radiogenic Ar content into the age equation. Using this approach, the effects of long-lasting burial and of detrital contamination are considered separately below.

MODELING K-AR AGES OF DIAGENETIC ILLITE BY GALOPER SIMULATION OF ILLITE CRYSTAL GROWTH MECHANISM

The model

In the simplest case, we ignore detrital contamination and consider only the effects of burial history and of the illitization mechanism on K-Ar dates. According to our current model (Środoń et al. 2000), illitization is treated as a process of nucle-

* E-mail: ndsrodon@cyf-kr.edu.pl

0003-004X/02/1112–1528$05.00

ation and growth of 2 nm thick crystals of illite ("fundamental particles," in the sense of Nadeau et al. 1984). It is not considered to be an Ostwald ripening process (Eberl et al. 1988; Inoue et al. 1988) or "permanent recrystallization" (Velde and Renac 1996). Therefore, no age information is lost due to dissolution of early formed small illite crystals, but the complete illitization history is retained in the illite crystals. For bentonites (Środoń et al. 2000), illitization proceeds in three subsequent steps: (1) nucleation of 2 nm thick crystals (100–75% smectite layers, hereafter %S, according to XRD measurement); followed by (2) simultaneous nucleation of new crystals (at a decaying rate) and growth of nucleated crystals by a surface-control mechanism (75–40%S); followed by (3) growth by the surface-control mechanism (<40%S) without simultaneous nucleation.

This 3-step mechanism leads to lognormal shapes for illite crystal-thickness distributions (CTDs) in bentonites.

In shales and in some other rocks (e.g., lacustrine Fe-illite-bearing sediments), "asymptotic" shapes of the CTDs are measured most often (unpublished data of D.D. Eberl; Dudek et al. 2002). This shape has been attributed to a constant-rate nucleation and growth phenomenon (Eberl et al. 1998; Kile et al. 2000). For shales, the shape has been explained, however, as composite, i.e., as the result of overlapping of illite-smectite and discrete illite crystal size distributions of diverse origin (Dudek 2001).

Illite CTDs resulting from different models of illitization can be simulated using the GALOPER computer program, which is based on the Law of Proportionate Effect (Eberl et al. 1998). When applied to crystal growth, this law states that the new size of a crystal after a growth cycle equals the previous size of the crystal plus the previous size of the crystal times a random number that varies between zero and one. After each such growth cycle (which corresponds to increasing time) for many crystals, the mean thickness of the distribution grows to a value N_n.

GALOPER also calculates the masses of illite crystals at subsequent steps during illitization, with the masses dependent on the path of the illitization reaction. If the timing of these steps were known, the mixed age, corresponding to a given reaction path, could be calculated. To express illitization (illite crystal growth) as a function of time, a relationship between N_n and time must be established. In our model, this relationship has been established as follows: (1) N_n was converted to XRD expandability (*%S*) using the set of following relationships, which have been established for bentonites (assumption is made that these relationships apply also to illite-smectites from shales, the relationships for which have not yet been investigated) (Środoń et al. 1992):

$$100/N_n = 100 - 100(FIX/0.9) \quad (1)$$

where *FIX* is the number of fixed K cations per half unit cell.

$$FIX = 0.079K_2O \quad (2)$$

(Clauer et al. 1997)

$$\%K_2O = 10.7 - 0.214\%S + 1.948e^{-3}(\%S)^2 - 8.889e^{-6}(\%S)^3 \quad (3)$$

(Środoń 2000)

(2) The relation between *%S* and temperature, given by Šucha et al. (1993, see their Fig. 3), was taken as representative of the illitization process in ordinary Al-rich shales, following the arguments of Środoń and Clauer (2001). Present-day temperatures of Šucha et al. (1993) were increased by 5 °C to convert to the maximum paleotemperatures characteristic of the basin they investigated (Clauer et al. 1997). The Šucha et al. figure corrected in this way gives *%S* (and thus N_n) reached by evolving illite-smectite at a given maximum paleotemperature. The relationship between N_n and maximum paleotemperature established in this way is presented in Figure 1. It is assumed in this model that the evolution of illite-smectite ended when the maximum paleotemperatures were reached.

With the aid of Figure 1, a thermal history of a basin (maximum paleotemperatures vs. time) can be converted into the evolution of illite crystal size through time (N_n vs. time). Table 1, columns 2, 3, and 5 present such data for two hypothetical thermal history models of a basin presented in Figure 2: (A) fast burial followed by slow burial, and (B) slow burial followed by fast burial, both reaching the onset of illitization (assumed as 70 °C), and the end of illitization (maximum paleotemperature), at the same time (40 and 10 Ma, respectively). GALOPER calculations were run to reach subsequent N_n values from Table 1. The masses of illite crystallized were calculated at each step, as were the mixed ages for each step, derived from the calculated amounts of K and radiogenic Ar in each mass of illite crystallized. The results of such calculations are given in Figure 2 and in Table 1. The details of the calculation are presented below.

The first cycle of GALOPER-simulated illitization (nucleation) was assigned the age of 40 Ma. After each subsequent cycle of nucleation and growth, new illite particles were created, and older particles were overgrown by new material. The cycle age (Table 1, columns 3 and 5) was assigned to the overgrowth material and newly nucleated crystals. The age of each overgrown crystal was treated as a mixed age and calculated as follows:

(1) K content of the nuclei were set to $0.45/O_{10}(OH)_2$ (one K interlayer per two silicate layers: Fig. 3). K content of the overgrowth was set to $0.9/O_{10}(OH)_2$ (one K interlayer per one silicate layer: Fig. 3). They were recalculated into $\%K_2O$ using

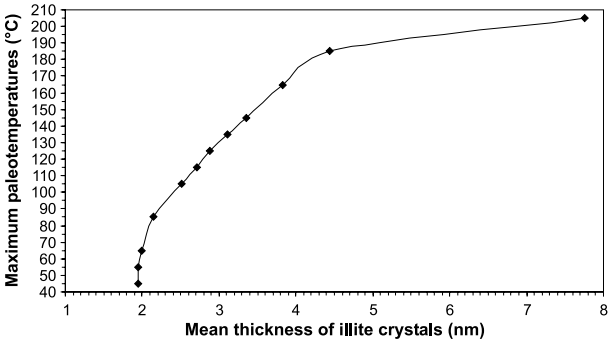

FIGURE 1. Relation between the mean thickness of illite fundamental particles and the maximum paleotemperatures, established by applying Equations 1–3 to Figure 3 of Šucha et al. (1993). This relation is used to model the mixed ages presented in Figure 2.

TABLE 1. Results of mixed K-Ar age calculation (columns 4 and 6) for illite-smectites undergoing illitization along two different thermal history paths shown in Figure 2

Cycle	N_n (nm)	Fast burial		Slow burial	
		Cycle age (Ma)	Calc. K-Ar age	Cycle age (Ma)	Calc. K-Ar age
		Decaying nucleation rate			
1	2.0	40.0	40.0	40.0	40.0
2	3.0	37.0	38.5	15.0	27.6
3	4.5	30.0	34.9	12.0	21.0
4	6.8	10.0	25.0	10.0	16.9
		Constant nucleation rate			
1	2.0	40.0	40.0	40.0	40.0
2	2.5	38.0	38.7	22.5	28.4
3	3.1	36.0	37.6	14.5	23.0
4	4.1	32.5	35.7	13.0	19.8
5	3.0	24.5	32.2	11.2	17.3
6	6.9	10.0	25.6	10.0	15.2

Notes: Reaction progress is modeled as GALOPER cycles (decaying and constant rate nucleation plus growth) and is expressed in the table as mean illite crystal thickness (N_n). The age of each cycle is established from N_n using Figures 1 and 2.

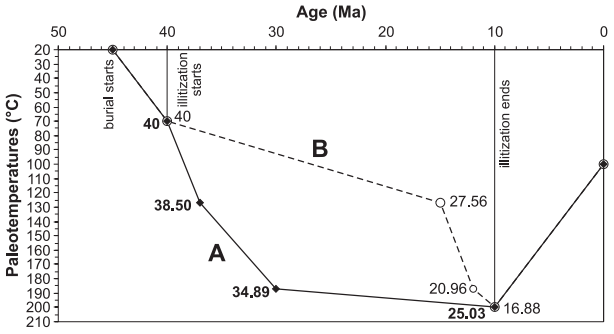

FIGURE 2. Two thermal history curves for samples deposited at 45 Ma, buried, then uplifted at 10 Ma (the end of illitization). These curves are used to model K-Ar mixed ages: (**A**) fast burial followed by slow burial, and (**B**) slow burial followed by fast. The mixed ages (in Ma), calculated using a decaying-rate nucleation mechanism (option 3 in GALOPER) are given in the figure for both curves (also in Table 1). As shown, case A ends up giving a date for its diagenetic illite-smectite of 25.03 Ma, compared to 16.88 Ma for case B.

Equation 2. (2) Radiogenic ^{40}Ar (Ar*) contents were back-calculated for the nuclei and for the overgrowth from their ages and $\%K_2O$ values by means of the standard K-Ar age equation:

$$\text{Age (Ma)} = 1880 \ln(1 + 9.07\text{Ar}^*/0.000119\%\text{K}) \quad (3)$$

%K and Ar* values for the i-th particle were calculated as weighted means:

$$\%K_i = \%K_{old}p_{old} + \%K_{new}(1 - p_{old}) \quad (4)$$
$$Ar^*_i = Ar^*_{old}p_{old} + Ar^*_{new}(1 - p_{old}),$$

where p_{old} is the mass fraction of old material (silicate layers) in a crystal (Fig. 3). (4) The age of each crystal was calculated from these weighted means. The mixed age of the sample (4th and 6th columns in Table 1) was calculated from $\Sigma\%K$ and ΣAr^*, where

$$\Sigma\%K = \Sigma\%K_i p_i \text{ and } \Sigma Ar^* = \Sigma Ar^*_i p_i \quad (5)$$

and p_i is the mass fraction of ith crystal in the whole sample. At the next cycle (overgrowth step), the previously calculated $\%K_i$ and $\%Ar^*_i$ were treated as the "old" values and the mixed age calculation was repeated.

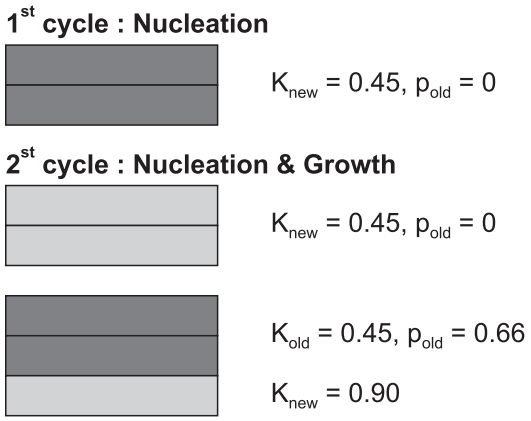

FIGURE 3. An illustration of the calculation (Eq. 4) of the mean K content for individual particles in the subsequent grow cycles. $0.9K/O_{10}(OH)_2$ is used for the K content of the illitic interlayer (Środoń et al. 1992); thus 0.45K is present if one illite interlayer corresponds to two silicate 2:1 layers (illite nucleus). p_{old} is the fraction of material from the previous calculation cycle.

Results of the model

Models were produced for both (1) the decaying nucleation rate, combined with the surface-controlled growth, and (2) the constant nucleation rate, combined with the surface-controlled growth. The results are presented as mixed ages at each calculation cycle (Table 1, Fig. 2) and as final distributions of crystal thickness and of ages of crystals with respect to their thickness (Fig. 4).

Conclusions for K-Ar dating of burial history

The mixed age at an intermediate stage of burial history in Figure 2 can be treated as equivalent to the final mixed age of a sample that had an identical burial history up until this stage, but was not buried to higher temperatures. The modeling clearly suggests a strong effect of burial history on the final illite age. The slow/fast burial history results in younger ages compared to the fast/slow burial path.

Whatever reaction mechanism has prevailed for a set of natural illites, it should be recognizable from the shapes of

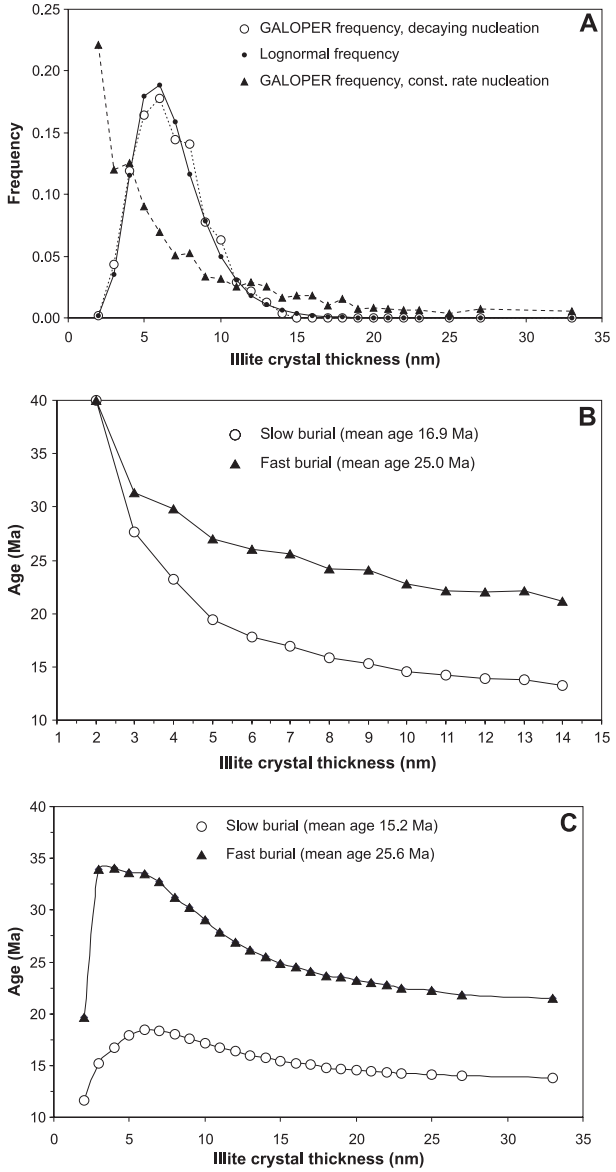

FIGURE 4. Results of modeling the crystal size distributions (**A**), and the distributions of mixed ages with respect to the crystal thickness for different combinations of thermal history and illitization mechanisms: (**B**) decaying nucleation rate and growth (**C**) constant nucleation rate and growth.

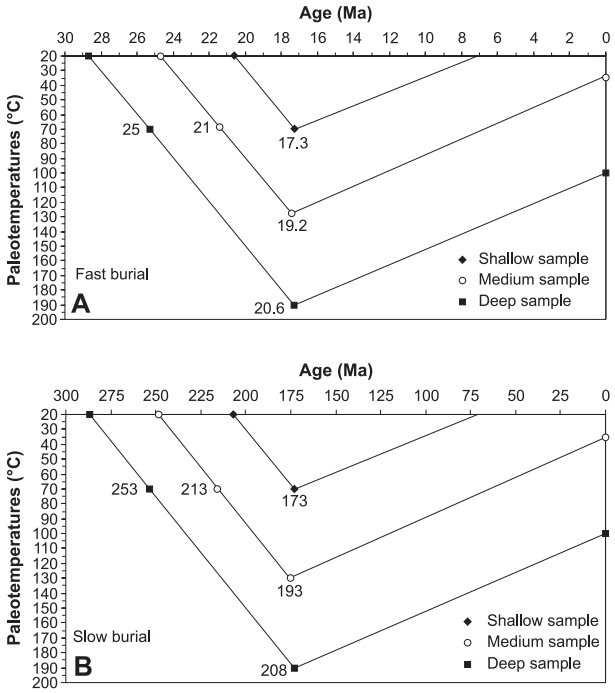

FIGURE 5. Thermal history curves for 3 depths from a single well in two hypothetical basins: (**A**) fast burial; (**B**) slow burial. For a given well, each of the three samples was buried to reach the onset of illitization (70 °C) at different times (shown in the figures), but reached their maximum paleotemperatures (end of illitization) at the same time. These curves are used to model the K-Ar age of the total diagenetically formed illite at the end of illitization ("the mixed diagenetic age" indicated by the bold numbers in each figure) using the decaying nucleation rate mechanism (option 3 in GALOPER). The shallow sample just reached the 70 °C isotherm, thus its onset age equals its end of illitization age. In the case of fast burial (**A**), the absolute difference in the final calculated ages between the shallow and the deep sample is small (3.3 Ma = "punctuated diagenesis"), while it is large for the slow burial case (**B**, 35 Ma). This figure illustrates how aspects of the burial history can be revealed from a set of K-Ar dates obtained from varying depths of a single well.

CTDs and the distributions of K-Ar ages with respect to the crystal size. The decaying-rate nucleation model gives a log-normal CTD (Fig. 4A) and older ages for the finest crystals (Fig. 4B). Constant-rate nucleation produces an asymptotic CTD (Fig. 4A) and younger ages for finer crystals (Fig. 4C).

Figure 2 implies that the diagenetic ages measured in a single vertical profile of a basin (borehole) should strongly depend on the burial history. Relevant modeling results for three samples from one vertical profile of a basin are presented in Figure 5. Fast burial (Fig. 5A) produces very close mixed ages (equivalent of "punctuated diagenesis" of Morton 1985), whereas slow burial (Fig. 5B) produces mixed ages increasing with depth. Thus single-well measurements can be indicative of the burial history. If reliable K-Ar dates are available from a sedimentary basin, this modeling approach can be used to verify its thermal history reconstruction.

Experimental evidence

For several K-bentonites, grain-size fractions containing illite crystals of different thickness have been dated (Table 2). These grain fractions were separated following the procedure of Clauer et al. (1997). The increase of *%S* and the decrease of $\%K_2O$ in finer fractions indicate that the mean thickness of illite crystals decreases in finer fractions (op.cit.). The data of Dong et al. (2000) for their bentonite no. 7773 reveal the same relationships.

The available dates are consistent with the decaying rate nucleation and growth mechanism recognized for K-bentonites:

TABLE 2. Available K-Ar dates for very fine particle size fractions of bentonite samples, containing populations of illite crystals of different thickness (Y < X of Clauer et al., 1997, are unspecified size fractions <0.1 μm)

Sample no. and fraction	wt%	K_2O	%*S*	Age (Ma ± 2μ)
Oligocene bentonites of the Carpathians (PhD thesis of M.Kotarba, personal information)				
CW	<0.02 μm	4.21		17.9 (1.1)
	0.02–0.05 μm	4.15		18.0 (1.7)
	0.05–0.1 μm	4.42		17.5 (1.6)
	0.1–0.2 μm	4.47		17.4 (1.2)
Kac.1	<0.02 μm	3.48		18.6 (2.0)
	0.02–0.05 μm	3.95		19.5 (2.5)
	0.05–0.2 μm	3.81		20.1 (2.6)
Hydrothermal Zempleni clay deposit (Clauer et al. 1997)				
	<Y μm	7.71	18	13.5 (0.5)
	X–0.1 μm	8.27	12	15.6 (0.5)
	0.1–0.2 μm	8.97	14	13.6 (0.4)
	0.2–0.3 μm	9.62	11	14.3 (0.5)
	>1 μm	8.44		14.0 (0.4)
Miocene bentonites of East Slovak Basin (Clauer et al. 1997)				
CIC1/20				
	<Y μm	2.32	66	7.4 (2.4)
	Y–X μm	4.18	49	7.1 (2.0)
	X–0.1 μm	3.88	54	3.7 (1.1)
TRH 1/37	<Y μm	6.63	28	8.1 (0.3)
	Y–X μm	7.14	22	7.9 (0.4)
	X–0.1 μm	7.76	14	10.2 (0.5)
Cretaceous bentonites of Montana (Clauer et al. 1997)				
Center of the bed	Y μm	3.62	54	42.5 (2.3)
	Y–X μm	5.50	39	42.4 (1.9)
	X–0.1 μm	5.07	32	41.1 (2.0)
Lower contact	<Y μm	3.51	48	63.9 (2.7)
	Y–X μm	6.15	29	50.5 (1.9)
	X–0.1 μm	6.43	30	50.1 (1.6)
Ordovician bentonites of the East European Craton (Środoń and Clauer, unpublished)				
POL-1	<0.02 μm	5.23		363 (10)
	0.02–0.05 μm	6.04		294 (08)
	0.05–2 μm	5.70		335 (09)
POL-2	<0.02 μm	5.56		360 (09)
	0.02–0.05 μm	5.71		341 (09)
	0.05–2 μm	5.28		346 (09)
POL-3	<0.02 μm	5.73		382 (10)
	0.02–0.05 μm	6.61		353 (09)

the dates are either equal (as is expected for short-lasting events) or the finer crystals are older, as is expected for a slow burial rate (Fig. 4B). In the extreme case (an Ordovician bentonite), the finest fraction is almost 70 Ma older then the coarser fraction (the coarsest is intermediate in age, which indicates aggregates). Equal ages for the various size fractions of a given sample in Table 2 are characteristic of fast burial (the Carpathian and one of the East Slovak Basin bentonites), for a hydrothermal event (Zempleni), and for the center of a thick bentonite bed (Montana). Analogous dates for shales are not available because of detrital contamination.

It must be emphasized that the data on these particular K-bentonites strongly affirm just how excellent a K-Ar clock illite-smectite is when crystals as small as <0.02 μm are so retentive of their radiogenic Ar.

The model presented in Figure 5 can be tested using data for bentonites coming from different depths of a single sedimentary basin. Data from the slowly subsiding (between 80 and 50 Ma) Denver Basin published by Elliot et al. (1991, see their Fig. 10) fulfill this criterion. The more-illitized samples are older (Fig. 6), as predicted by the model of a relatively slow-burial basin (Fig. 5B). As concluded by Elliot et al. (1991), their data indicate that diagenetic illite is not undergoing recrystallization, which is in agreement with our nucleation and growth model.

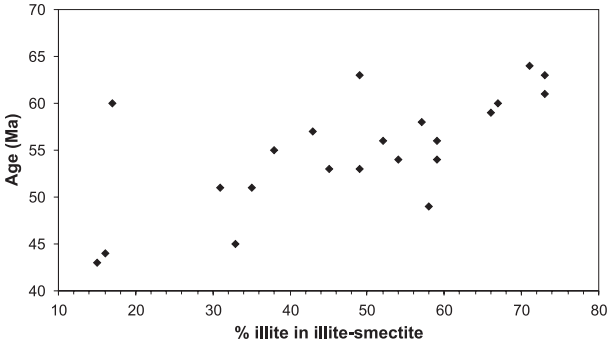

FIGURE 6. Data of Elliot et al. (1991) for illite-smectites from bentonites from the Denver Basin, documenting the K-Ar mixed age trend predicted by Figure 5B. The %I in illite-smectite is a proxy for the maximum paleotemperatures, and ca. 20 Ma difference in age is indicative of a slow burial scenario (Fig. 5B).

INTERPRETATION OF K-AR DATES OF MIXTURES OF DIAGENETIC AND DETRITAL ILLITE

Cases for consideration

Clay fractions of common rocks that have undergone diagenesis are mixtures of a detrital component and an authigenic component. Possible approaches for extracting the end-member ages from the dates of clays of mixed origins depend on the availability of an accurate mineral composition for the studied sample. Three cases can be treated separately: (1) The absolute amounts of both the detrital and the diagenetic components are known. This case implies that the ratio of the two components has been measured accurately (e.g., as $2M_1/1M_d$ polytype ratio: Grathoff and Moore1996; Grathoff et al. 1998), and, equally important, that other K minerals are absent, K-free minerals are absent or have been quantified. Under such conditions, both K and radiogenic Ar contents of the end-member components can be evaluated separately, by applying the linear extrapolation method to the relevant measurements of a few grain size fractions. Both the detrital and the diagenetic age can be calculated from the extrapolated numbers. An example of such a calculation was given by Środoń (1999b, Fig. 3) and the experimental evidence is provided here as Figure 7A. It presents the measurements of $\%K_2O$ and radiogenic Ar content performed on a set of artificial mixtures of pure Miocene illite (high % K_2O) and Triassic illite/smectite (low % K_2O). Samples were wet-mixed ultrasonically and then freeze-dried and homogenized in a mortar. The measurement technique was described in Clauer et al. (1997). The K_2O and radiogenic Ar vs. mixture composition ("fraction old clay") plots are strictly lin-

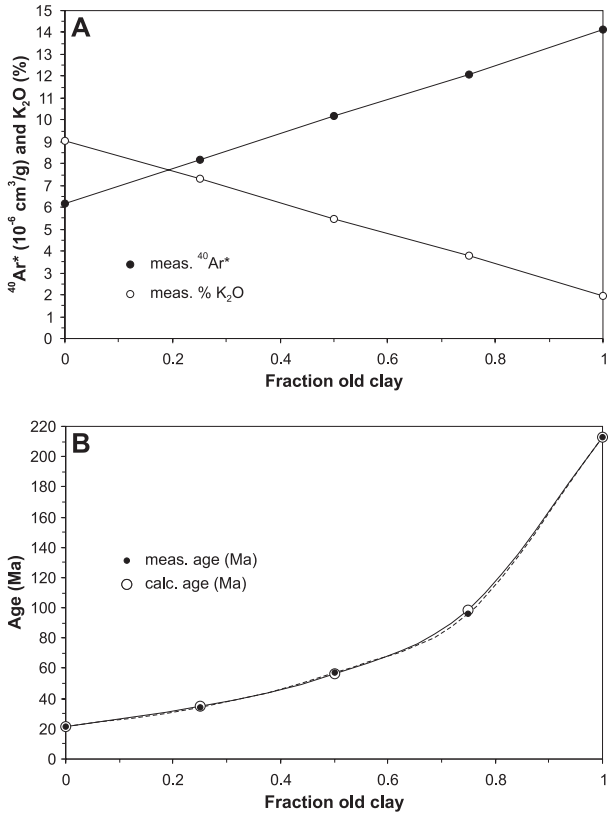

FIGURE 7. K-Ar data for artificial mixtures of a 22 Ma illite and a 213 Ma illite-smectite, verifying the theoretical approach to modeling mixtures used in this study (Środoń 1999b). Measured K_2O (%) and radiogenic ^{40}Ar* values (in 10^{-6}cm^3/g) are shown in Figure 7A, and measured and calculated mixed ages in 7B.

ear, as expected. (2) A second case is where only the ratio of the detrital vs. the diagenetic components is available (contaminants not quantified). Here, the mixed age extrapolation technique must be used. Mixed age plots are not linear (Środoń 1999b, 2000; Ylagan et al. 2000), thus successful extrapolation requires the mixed age data covering the entire range from close to 100% detrital to ca. 100% diagenetic (appropriate set of grain size fractions; otherwise the curvature cannot be evaluated properly). An example attempting to provide such extrapolation on natural shales was given by Aronson (2000). Figure 7B presents an experimental verification of this approach on the same artificial mixtures of two illites of different age and different K_2O content as used in Figure 7A. As expected, the mixed age plot is a curve. The measured mixed ages (open circles) are matched almost perfectly by the calculated mixed ages (filled triangles), obtained by applying the age function to the mean values of K_2O and ^{40}Ar, calculated from the extrapolated end-member values (Środoń 1999b). (3) The third case considered is when the ratio of the detrital to the diagenetic component is not available (e.g., both include 1M_d polytypes that cannot be distinguished). In such a case, an approach based on selective K extraction from one of the components can be tried (Chaudhuri et al. 1999). Alternatively, the mixed ages can be modeled using available mineralogical data, and the geological feasibility of the model can be judged. An example of such a procedure is presented below.

Modeling approach

The classic data of Aronson and Hower (1976) and Hower et al. (1976) for shales from the CWRU 6 well of the U.S Gulf Coast, which have been interpreted and commented on by many later authors (Boles and Franks 1979; Odin 1982; Morton 1985; Ohr et al. 1991; Eberl 1993; Clauer et al. 1995), are used to illustrate our modeling approach. The measured K and radiogenic Ar contents of the <0.1 μm fractions vs. depth were modeled using versions of Equations 4, which accounts for other minerals present in a sample:

$$\%K = \%K_{dtI}p_{dtI} + \%K_{dtIS}p_{dtIS} + \%K_{dgIS}p_{dgIS}$$
$$Ar^* = Ar^*_{dtI}p_{dtI} + Ar^*_{dtIS}p_{dtIS} + Ar^*_{dgIS}p_{dgIS} \quad (6)$$

where p_{dtI}, p_{dtIS}, and p_{dgIS} are the mass fractions of the detrital illite, detrital illite-smectite, and diagenetic illite-smectite, respectively. The samples also contain kaolinite, thus:

$$p_{dtI} + p_{dtIS} + p_{dgIS} + p_{kao} = 1 \quad (7)$$

The percent K in detrital illite ($\%K_{dtI}$) was calculated (Eq. 2) from 7% K_2O in the Gulf Coast illite given by Hower et al. (1976). The sum of $\%K_{dtIS}$ + $\%K_{dgIS}$ was calculated via K_2O from %*S* given by Hower et al. (1976) using Equation 3, which gives an experimental relationship between %*S* and K_2O in illite-smectites (illite-smectite in Gulf Coast shales is partially detrital and partially diagenetic). The calculated number was adjusted (lowered) to allow for NH_4 substitution in illitic layers (Cooper and Abedin 1981; Lindgreen et al. 2000). Then $\%K_{dtIS}$ was obtained from Equation 3, assuming 80%*S* in the detrital illite-smectite (Hower et al. 1976). The $\%K_{dgIS}$ was calculated as the difference between total %K in illite-smectite and $\%K_{dtIS}$.

Given the %K values, the corresponding Ar* values for the three clays were back-calculated by the standard age equation, from their estimated ages: 420 Ma for the detrital illite (Weaver and Wampler 1970), 60 Ma for the detrital illite-smectite, and 18 Ma for the diagenetic illite-smectite (Aronson and Hower 1976).

The value of p_{kaol} was taken from Hower et al. (1976). The sum of p_{dtIS} + p_{dgIS} was the second adjustable parameter in the model (along with the NH_4 content of illitic layers in illite-smectite). Having chosen the sum, p_{dtIS} and p_{dgIS} were calculated from the sum and the expandabilities (total and 80%*S* of the detrital I-S), and p_{dtI} was calculated as the difference from Equation 7.

An Excel spreadsheet was used to perform the calculations. For each of the <0.1 μm samples of Aronson and Hower (1976), the fraction of illite-smectite and its K content were individually adjusted to match the two independent variables: measured %K and measured ^{40}Ar*.

RESULTS

Figure 8 presents the results of this modeling, and Figure 9 demonstrates the variation of measured (%kaolinite) and calculated (%illite-smectite and %illite) compositions of the <0.1 µm fractions with depth in the CWRU 6 well. The published, experimentally measured %K and ^{40}Ar* contents were modeled very closely by varying the illite-smectite content of the <0.1 µm fraction between 70 and 80%. As a result, a slight increase (within the 15–20% range) in detrital illite is produced by the calculation, simultaneous with the measured decrease in kaolinite down the well. To obtain a good fit, the %K content of illite-smectite had to be lowered to 70–80% of the value calculated from *%S* using Equation 3 and 2.

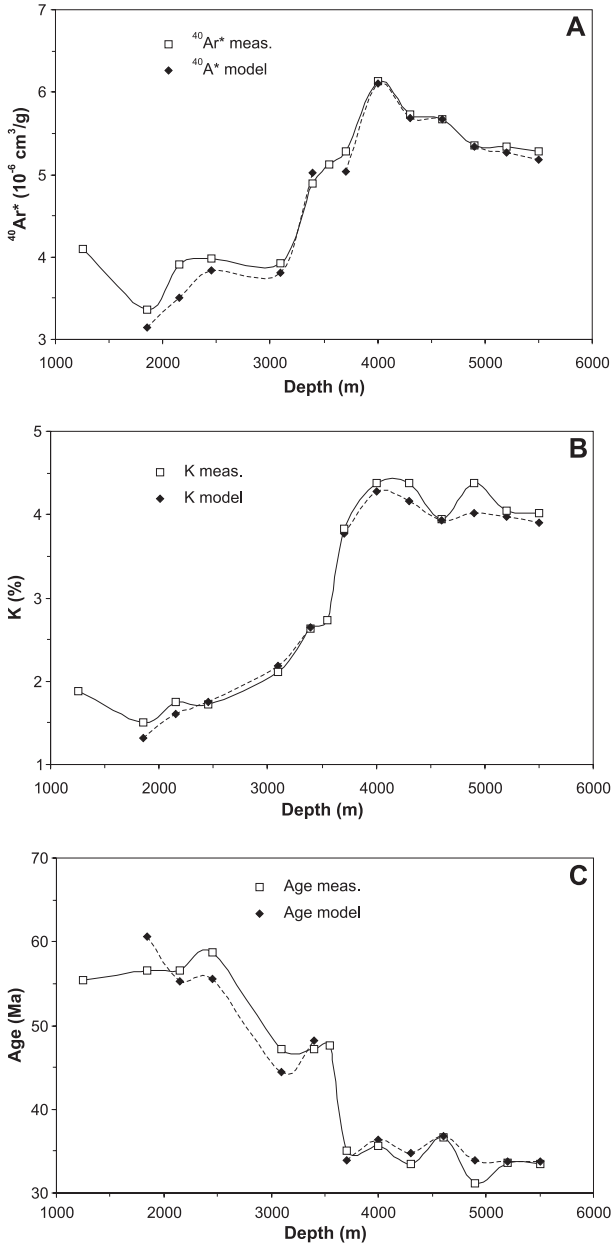

FIGURE 8. The results of modeling K-Ar data of <0.1 µm fractions from the shales of CWRU 6 well (Aronson and Hower 1976): (**A**) ^{40}Ar* (in 10^{-6}cm^3/g), (**B**) % K, (**C**) age (Ma).

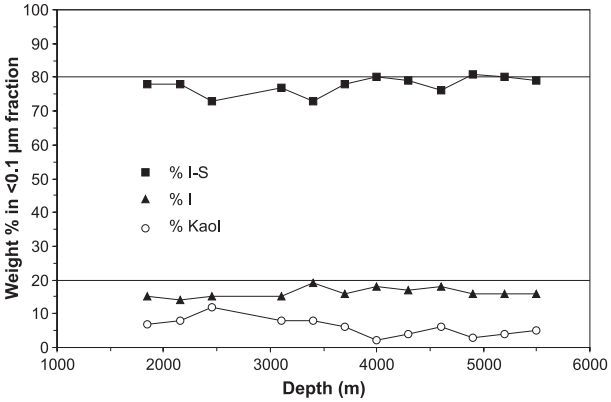

FIGURE 9. Measured (% kaolinite) and calculated (% illite-smectite and % illite) composition of <0.1 µm fraction from the shales of CWRU 6 well, used in the model presented in Figure 8.

Evaluating diagenetic ages in the presence of detrital illite

The mixed age calculation of Środoń (1999b) has been verified experimentally by dating artificial mixtures and used to model classic K-Ar and mineralogical data from CWRU 6 well of the Gulf Coast. The task performed with the aid of an Excel spreadsheet is equivalent to solving two equations (Eq. 6) with two unknowns (the fraction of illite-smectite in the sample and the %K in illite-smectite). Consequently, the solution presented in Figure 8 is unique for the accepted set of input data and its accuracy depends on the accuracy of the input data. The calculated subtle increase of contents of illite and illite-smectite down the profile, going along with the observed decrease in kaolinite, may be of sedimentary origin, being consistent with the regressive character of the sequence (Hower et al. 1976).

The reported modeling exercise indicates that the K-Ar data for the CWRU 6 well can be fully explained by burial diagenetic illitization, which overprints a subtle trend in detrital mineral content, presumably of sedimentary origin.

ACKNOWLEDGMENTS

Clarity and language of the presentation benefited from reviews by Jim Aronson, Dewey Moore, and Dougal McCarty.

REFERENCES CITED

Aronson, J.L. and Farrington, S.A. (2000) Origin of 2M and 1M illite in the Devonian shales of the Appalachian basin. Geological Society of America Annual Meeting Abstracts, A366.

Aronson, J.L. and Hower, J. (1976) The mechanism of burial metamorphism of argillaceous sediments: 2. radiogenic argon evidence. Geological Society of America Bulletin, 87, 738–744.

Aronson, J.L. and Lee M.C. (1986) K/Ar systematics of bentonite and shale in a contact metamorphic zone, Cerrillos, New Mexico. Clays and Clay Minerals, 34, 483–487.

Boles, J.R. and Franks, S.G. (1979) Clay diagenesis in Wilcox sandstones of southwest Texas; implications of smectite diagenesis on sandstone cementation. Journal of Sedimentary Petrology, 49, 55–70.

Chaudhuri, S., Środoń, J., and Clauer, N. (1999) K-Ar dating of the illitic fractions of Estonian "blue clay" treated with alkylammonium cations. Clays and Clay Minerals, 47, 96–102.

Clauer, N. and Chaudhuri, S. (1995) Clays in Crustal Environments. Isotope Dating and Tracing, 359 p. Springer-Verlag, Berlin.

Clauer, N., Furlan, S., and Chaudhuri, S. (1995) The illitization process in deeply buried shales of the Gulf Coast area. Clays and Clay Minerals, 43, 257–259.

Clauer, N., Środoń, J., Francu, J., and Šucha, V. (1997) K-Ar dating of illite fundamental particles separated from illite-smectite. Clay Minerals, 32, 181–196.

Cooper, J.E. and Abedin, K.Z. (1981) The relationship between fixed ammonium-nitrogen and potassium in clays from a deep well on the Texas Gulf Coast. Texas Journal of Science, 33, 103–111.

Dong, H., Hall, C.M., Peacor, D.R., Halliday, A.N., and Pevear, D.R. (2000) Thermal $^{40}Ar/^{39}Ar$ separation of diagenetic from detrital illitic clays in Gulf Coast shales. Earth and Planetary Science Letters, 175, 309–325.

Dudek, T. (2001) Diagenetic evolution of illite/smectite in the Miocene shales from the Przemyśl area (Carpathian Foredeep). PhD thesis, 148 p. Institute of Geological Sciences PAN, Kraków.

Dudek, T., Środoń, J., Eberl, D.D., Elsass, F., and Uhlik, P. (2002) Thickness distribution of illite crystals in shales. Part I: XRD vs. HRTEM measurements. Clays and Clay Minerals, in press.

Eberl, D.D. (1993) Three zones for illite formation during burial diagenesis and metamorphism. Clays and Clay Minerals, 41, 26–37.

Eberl, D.D. and Środoń, J. (1988) Ostwald ripening and interparticle diffraction effects for illite crystals. American Mineralogist, 73, 1335–1345.

Eberl, D.D., Drits V., and Środoń, J. (1998) Deducing growth mechanisms for minerals from the shapes of crystal size distributions. American Journal of Science, 298, 499–533.

Elliot, W.C., Aronson, J.L., Matisoff, G., and Gautier, D.L. (1991) Kinetics of the smectite to illite transformation in the Denver Basin: clay mineral, K-Ar data, and mathematical model results. American Association of Petroleum Geologists Bulletin, 75, 436–462.

Grathoff, G.H. and Moore, D.M. (1996) Illite polytype quantification using WILDFIRE© calculated X-ray diffraction patterns. Clays and Clay Minerals, 44, 835–842.

Grathoff, G.H., Moore, D.M., Hay, R.L., and Wemmer, K. (1998) Illite polytype quantification and K/Ar dating of Paleozoic shales: a technique to quantify diagenetic and detrital illite. In J. Schiebler, W. Zimmerle, and P. Sethi, Eds., Shales and Mudstones. II., p161–175. E. Schweizerbartšche Verlagsbuchhandlung, Stuttgart.

Hower, J., Eslinger, E.V., Hower, M.E., and Perry, E.A. (1976) Mechanism of burial metamorphism of argillaceous sediments: 1. Mineralogical and chemical evidence. Geological Society of America Bulletin, 87, 725–737.

Hunziker, J.C., Frey, M., Clauer, N., Dallmeyer, R.D., Friedrichsen, H., Flehmig, W., Hochstrasser, K., Roggwiller, P., and Schwander H. (1986) The evolution of illite to muscovite: mineralogical and isotopic data from the Glarus Alps, Switzerland. Contributions to Mineralogy and Petrology, 92, 157–180.

Inoue, A., Velde, B., Meunier, A., and Touchard, G. (1988) Mechanism of illite formation during smectite-to-illite conversion in a hydrothermal system. American Mineralogist, 73, 1325–1334.

Kile, D.E., Eberl, D.D., Hoch, A.R., and Reddy, M.M. (2000) An assessment of calcite crystal growth mechanisms based on crystal size distributions. Geochimica et Cosmochimica Acta, 64, 2937–2950.

Lindgreen, H., Drits, V.A., Sakharov, B.A., Salyn, A.L., and Dainyak, L.G. (2000) Illite-smectite structural changes during metamorphism in black Cambrian Alum Shales from the Baltic area. American Mineralogist, 85, 1223–1238.

Morton, J.P. (1985) Rb-Sr evidence for punctuated illite/smectite diagenesis in the Oligocene Frio Formation: Geological Society of America Bulletin, 96, 114–122.

Mossman, J.-R. (1991) K-Ar dating of authigenic illite/smectite material: application to complex mixtures of mixed-layer assemblages. Clay Minerals, 26, 189–198.

Nadeau, P.H., Wilson, M.J., McHardy, W.J., and Tait, J. (1984) Interstratified clay as fundamental particles. Science, 225, 923–925.

Odin, G.S. (1982) Effect of pressure and temperature on clay mineral potassium-argon ages. In G.S. Odin, Ed., Numerical Dating in Stratigraphy, p. 307–319. Wiley, New York.

Ohr, M., Halliday, A.N., and Peacor, D.R. (1991) Sr and Nd isotopic evidence for punctuated clay diagenesis, Texas Gulf Coast. Earth and Planetary Science Letters, 105, 110–126.

Pevear, D.R. (1992) Illite age analysis, a new tool for basin thermal history analysis. In Y.K. Kharaka and A.S. Maest, Eds., Proc. 7th International Symposium on Water-Rock Interactions, p. 1251–1254. Balkema, Rotterdam.

Środoń, J. (1999a) Nature of mixed-layer clays and mechanisms of their formation and alteration. Annual Review of Earth and Planetary Sciences, 27, 19–53.

——— (1999b) Extracting K-Ar ages from shales: a theoretical test. Clay Minerals, 33, 375–378.

——— (2000) Reply to discussion of "Extracting K-Ar ages from shales: a theoretical test". Clay Minerals, 35, 605–608.

Środoń, J. and Clauer, N. (2001) Diagenetic history of Lower Paleozoic sediments in Pomerania (northern Poland) traced across the Teisseyre-Tornquist tectonic zone using mixed-layer illite-smectite. Clay Minerals, 36, 15–27.

Środoń, J., Elsass, F., McHardy, W. J., and Morgan, D. J. (1992) Chemistry of illite/smectite inferred from TEM measurements of fundamental particles. Clay Minerals, 27, 137–158.

Środoń, J., Eberl, D.D., and Drits, V.A. (2000) Evolution of fundamental particle-size during illitization of smectite and implications for reaction mechanism. Clays and Clay Minerals, 48, 446–458.

Šucha, V., Kraus, I., Gerthofferova, H., Petes, J., and Serekova, M. (1993) Smectite to illite conversion in bentonites and shales of the East Slovak Basin. Clay Minerals, 28, 243–253.

Velde, B. and Renac, C. (1996) Smectite to illite conversion and K-Ar ages. Clay Minerals, 31, 25–32.

Weaver, C.E. and Wampler, J.M. (1970) K, Ar, illite burial. Geological Society of America Bulletin, 81, 3423–3430.

Ylagan, R.F., Pevear, D.R., and Vrolijk, P.J. (2000) Discussion of "Extracting K-Ar ages from shales: a theoretical test." Clay Minerals, 35, 599–604.

MANUSCRIPT RECEIVED JULY 3, 2001
MANUSCRIPT ACCEPTED JULY 13, 2002
MANUSCRIPT HANDLED BY JAMES ARONSON